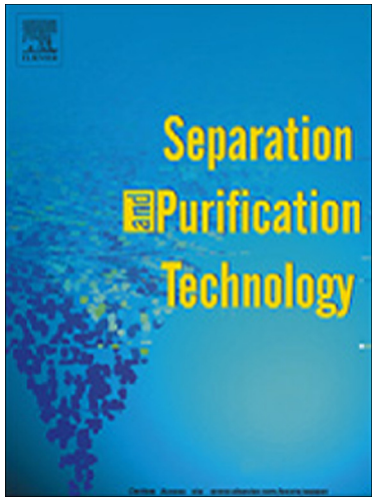

Hybrid Chitosan/$FeCl_3$ Coagulation-Membrane Processes: Performance Evaluation and Membrane Fouling Study in Removing Natural Organic Matter

W.L. Ang, A.W. Mohammad, Y.H. Teow, A. Benamor, N. Hilal

PII: S1383-5866(15)30121-0
DOI: http://dx.doi.org/10.1016/j.seppur.2015.07.053
Reference: SEPPUR 12472

To appear in: *Separation and Purification Technology*

Received Date: 11 March 2015
Revised Date: 22 July 2015
Accepted Date: 24 July 2015

Please cite this article as: W.L. Ang, A.W. Mohammad, Y.H. Teow, A. Benamor, N. Hilal, Hybrid Chitosan/$FeCl_3$ Coagulation-Membrane Processes: Performance Evaluation and Membrane Fouling Study in Removing Natural Organic Matter, *Separation and Purification Technology* (2015), doi: http://dx.doi.org/10.1016/j.seppur.2015.07.053

Hybrid Chitosan/$FeCl_3$ Coagulation-Membrane Processes: Performance Evaluation and Membrane Fouling Study in Removing Natural Organic Matter

W.L. Ang[a], A. W. Mohammad [a,b*], Y.H. Teow[a], A. Benamor[c], N. Hilal[d]

[a] Department of Chemical and Process Engineering, Faculty of Engineering and Built Environment, Universiti Kebangsaan Malaysia, 43600 Bangi, Selangor Darul Ehsan, Malaysia.
[b]Centre for Sustainable Process Technology (CESPRO), Faculty of Engineering and Built Environment, Universiti Kebangsaan Malaysia, 43600 Bangi, Selangor Darul Ehsan, Malaysia.
[c]Gas Processing Center, Qatar University, Doha, Qatar
[d]Centre for Water Advanced Technologies and Environmental Research (CWATER), College of Engineering, Swansea University, Swansea SA2 8PP, UK

*Corresponding author. Tel: +603-89216410; Fax: +603-89216148; E-mail: wahabm@eng.ukm.my

Abstract:

Coagulation is the most common process used to remove the natural organic matter (NOM) for clean water supply and safe consumption. However, most of the time, the supernatant water quality produced did not meet the drinking water standard and several dispute issues currently exist about the impact of conventional inorganic coagulants on the environment and living organisms. In this study, hybrid coagulation-membrane processes were implemented for NOM treatment using chitosan as a natural coagulant. Its performance in terms of turbidity and humic acid (HA) removal was tested and compared with inorganic ferric chloride ($FeCl_3$) coagulant. It was discovered that both coagulants were capable to remove 90% of the HA and produce supernatant water with acceptable quality for membrane processes; both nanofiltration (NF) and reverse osmosis (RO) membrane processes managed to remove nearly all of the turbidity and HA in the water. However, a hybrid process using chitosan had a more severe effect on membrane fouling compared to $FeCl_3$ coagulation pre-treatment processes due to the smaller and neutral particles produced by chitosan coagulation, forming a compact foulant layer on the membrane surface. Therefore, the wise selection of a coagulant for the hybrid coagulation-membrane process is crucial for attaining high removal efficiency and low fouling propensity.

Keywords: Hybrid coagulation-membrane process, Membrane fouling mechanism, Nanofiltration, Reverse osmosis, NOM removal in water treatment

1. Introduction

Natural organic matter (NOM) is a common substance found in natural freshwater which needs to be removed before the water can be used for daily consumption. Humic acid (HA) is one of the major components of NOM. The presence of HA in water source not only impart colour to water, but also contribute to the formation of carcinogenic disinfection-by-products (DBPs) when it reacts with ozone, chlorine or chlorine based disinfectant in conventional water treatment process [1,2]. These DBPs are carcinogens, as direct exposure to them may led to cancers, miscarriages, and nervous system complications [3]. Therefore, the effective and economic removal of HA from water has become a very challenging task in the current development of water purification technologies.

The coagulation process is one of the most common techniques employed to remove NOM in raw water [4]. The conventional coagulants generally fall into two categories: those based on aluminium and those based on iron [5,6]. Coagulation preferentially removes the higher molecular weight, more hydrophilic, and more acidic constituent of dissolved organic matter (DOM). Therefore, NOM with high molecular weight has been found to be able to associate with Al (III) or Fe (IIII) salt in the coagulation process [7,8]. However, there is vital concern regarding the ingestion of high concentrations of metal coagulants in treated water, which will potentially cause adverse health effects [5,9]. Hence, the application of a natural coagulant appears to be an attractive option for the replacement of conventional chemical coagulants.

Chitosan is a non-toxic, biodegradable, renewable, and environmentally friendly biopolymer coagulants that can be used in the coagulation process [5,10]. Studies were carried out to investigate the performance of chitosan in the coagulation process by comparing it with other conventional chemical coagulants [11–13]. It has been proven that chitosan was capable to remove colloid particles and HA from water [5,13–17]. As reported by Bratskaya et al. [17], chitosan ionic forms were able to remove 50 mg/L HA up to 95-100%. Coagulation process is capable of removing much of the NOM in water, but it could not remove all the dissolved NOM (residual NOM capable to form carcinogenic disinfection by-products) and emerging pollutants such as toxins, pesticides, pharmaceutical residues, arsenic, and herbicides. Hence, in order to

produce drinking water that meets the required standard, further treatment after coagulation process is required [18].

Membrane technology is a dignified separation technology and has been widely implemented for the production of process water from groundwater, surface water or wastewater as a valuable means of filtering in the water industry [19]. Progress has been made with regards to the use of two major pressure-driven membrane processes, nanofiltration (NF) and reverse osmosis (RO) as an alternative technology to conventional treatment in separating HA particles from the water source to meet more stringent water quality regulations [20–22]. However, despite the expansion and successful application of membrane systems in the water industry, a decline in membrane performance over a period of time towards a high susceptibility fouling effect is still a critical problem in the water industry. It demands considerable attention, as it affects separation properties and increases the operational pressure, which leads to higher operational costs due to occasional membrane replacement (membrane replacement involves 20-30% of the operating cost), thus constraining the widespread application of membrane technology for HA separation in water treatment processes [23]. Consequently, current research and development in membrane technology are focused on these problems and directed towards the development of hybrid coagulation-membrane processes [18]. Coagulation applied as a pre-treatment prior the membrane filtration unit will reduce the amount of foulants in the raw water and thus decrease the membrane fouling propensity while improving the water quality produced.

Successful implications of coagulation-ultrafiltration/microfiltration (UF/MF) in water treatment plants have been reported elsewhere [24–32]. However, these hybrid processes could not remove all of the foulant, especially low molecular weight NOM [26,33,34]. Hence, the integration of NF/RO processes with coagulation pre-treatment is proposed for effective removal. Besides, many of the chitosan studies were carried out on coagulation processes solely, whereby the effect of chitosan coagulation on NF/RO membrane performance has not been well investigated. Therefore, in the present work, the potential of chitosan as a coagulant in hybrid coagulation-NF/RO membrane processes to remove NOM and turbidity in water has been explored. For the application of feasibility, comparison study with conventional inorganic Fe-based coagulant, ferric chloride ($FeCl_3$) was also carried out.

2. Experimental

2.1. Chemicals and membranes

All of the chemicals used were analytical grade, unless stated otherwise. HA, chitosan, kaolin, acetic acid, and ferric chloride ($FeCl_3$) were purchased from Sigma Aldrich (Malaysia). Ultrapure (UP) water with a quality of 18 $M\Omega cm^{-1}$ was used for all solution preparation. Chitosan was dissolved in 1% acetic acid solution while $FeCl_3$was dissolved in UP water. Membranes used in this study were NF 270 and XLE purchased from Dow Filmtec (USA). The properties of the membranes used are shown in Table 1.

Table 1
Properties of NF 270 and XLE membranes used in the study

Membranes	Class[a]	Molecular weight cut-off (MWCO) (Da)[a]	Root mean square (RMS) roughness (nm)[b]	Zeta potential at pH 9 (mV)[b]
NF 270	NF	200~400	9.0 ± 4.2	-41.3
XLE	Brackish water reverse osmosis (BWRO)	~100	142.8 ± 9.6	-27.8

[a] Information provided by the manufacturer [35]
[b] Zeta potential values and RMS roughness taken from [36]

2.2. Preparation of synthetic feed water

Synthetically prepared water with fixed turbidity was used in this work. It was prepared by dissolving a pre-weighed amount (0.1 g) of HA powder in 10 ml of 0.1 M sodium hydroxide (NaOH) solution under continuous stirring for around 1 hour to ensure the complete dissolution of HA. Five litres of UP water was then added into the completely dissolved HA solution to alter the HA concentration to 20 ppm. A suitable amount of kaolin was added into the synthetic water to adjust its turbidity to 30 ± 0.5 NTU. The pH of the water was adjusted to 7 by using NaOH and hydrochloric acid (HCl) solution. The characteristics of the synthetic water are shown in Table 2.

Table 2
Quality parameters of the synthetic feed water

Parameters	pH	Conductivity (μS)	UV_{254} (cm^{-1})	Zeta potential (mV)	Turbidity (NTU)
Values	7±0.1	22±1	0.65±0.03	-50±1	30±0.5

2.3. Jar test coagulation

Coagulation pre-treatment prior to membrane processes was carried out in a conventional jar test apparatus (Model ZR4-6, Zhongrun Water, China). The coagulation procedures consist of three steps: vigorous stirring after the addition of coagulant (100 rpm for 1 minute), mild stirring (30 rpm for 29 minutes), and settling (30 minutes). The dosage of chitosan and $FeCl_3$ was varied in order to obtain the optimal dosage which results in the highest removal rate of turbidity and HA (represented by UV_{254} reading) from the raw testing water. The supernatant obtained after the coagulation process was then used as the feed water for membrane filtration. The removal efficiency of foulant was calculated using the following equation:

$$R = \left(\frac{c_i - c_f}{c_i} \right) \times 100\% \quad (1)$$

Where R denotes the rejection efficiency of the foulant (%), c_i indicates the initial HA concentration, and c_f indicates the final HA concentration after the coagulation process.

2.4. Cross-flow permeation system

Fig. 1 shows the schematic diagram of bench-scale cross-flow membrane experimental setup with a recycle loop. All commercial flat sheet membranes were cut into rectangular shapes and laid on top of the CF 042 membrane holder (Sterlitech, USA) in the membrane test cell with membrane effective filtration area of 0.0042 m^2 (excluding the area covered by the O-ring) and tightened by a rubber O-ring.

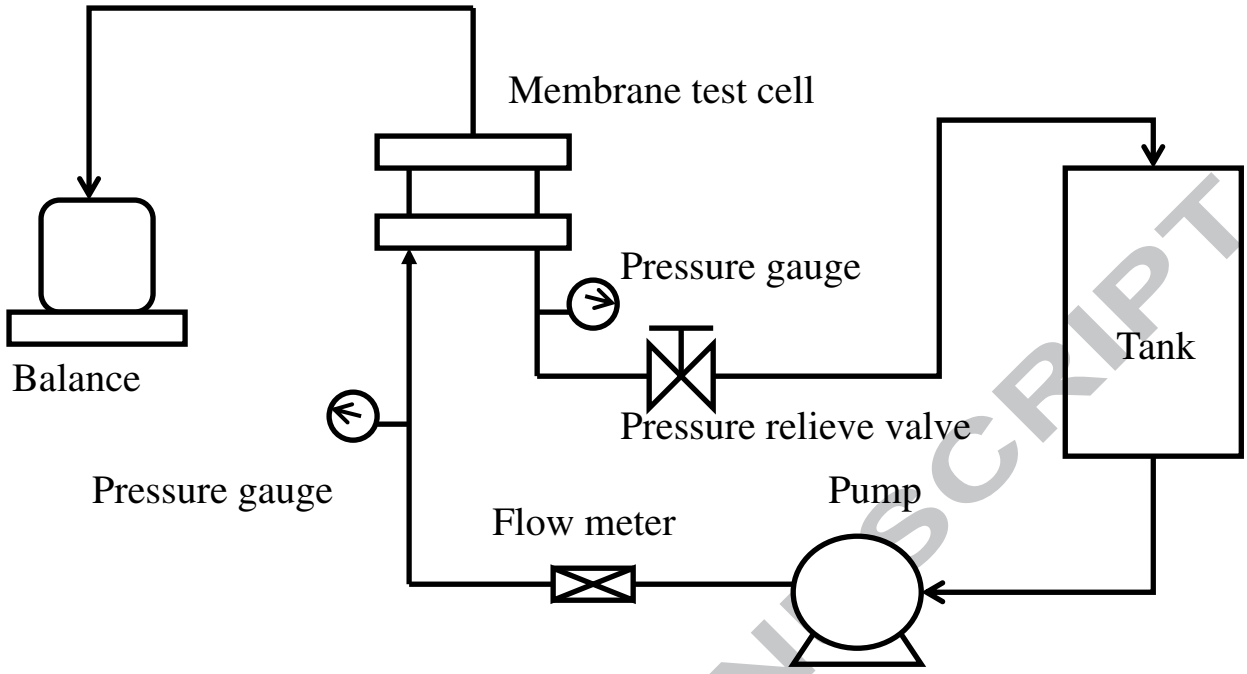

Fig. 1. Schematic diagram of bench-scale cross-flow filtration process.

Before starting the filtration experiment, the newly cut membrane was soaked in UP water and left for a day to ensure the complete removal of residual solvent/chemical from the membrane. In order to alleviate the impact of compaction, pre-filtration study with UP water was first conducted at a constant pressure of 15 bars for 1 hour until a steady-state flux was achieved.

During the membrane filtration experiment, supernatant solution from coagulation process was discharged into the feed tank and kept at a constant temperature of 27ºC. A flow meter was installed at the feed stream to monitor the flow rate of the feed solution. The applied pressure of the filtration system was generated using the high pressure pump (Blue Clean, BC 610, Italy) and controlled at 10 bars, while the retentate from the membrane system was re-circulated to the feed tank at a constant cross-flow rate per unit projection membrane area of 42 cm/s to minimise the changes of feed concentration. Two pressure gauges were used to indicate the operating pressure of the feed and retentate streams. To obtain insights into the fouling behaviour, the membrane filtration experiment was conducted for 5 hours. In each experimental run, fresh synthetic water was prepared and added into the feed tank of the cross-flow filtration unit. Foulants attached on the membranes were extracted by soaking the membranes in 0.1 M NaOH solution.

The permeate flux (J) was determined by direct measurement of the permeate volume over the permeation time:

$$J = \frac{V}{At} \tag{2}$$

where J is the permeate flux, V is the permeate volume, A is the membrane effective surface area, and t is the time taken to collect the permeate.

2.5. Resistance in series model and fouling index

Resistance in series model was used to estimate the total resistance of the filtration experiment [20,37]:

$$J = \frac{\Delta P}{\eta(R_m + R_a + R_p + R_c)} = \frac{\Delta P}{\eta R_t}, \tag{3}$$

where J is the permeate flux, ΔP is the trans-membrane pressure (TMP), η is the dynamic viscosity, and R_t denotes the total resistance due to membrane hydraulic resistance (R_m), adsorption resistance (R_a), pore blocking resistance (R_p) and cake layer resistance (R_c). R_t was measured from the operational data that were obtained from HA filtration solution using Eq. (3). R_m was measured by filtering UP water through a new membrane at a constant pressure assuming R_p, R_c, and R_a to be zero. With the known ΔP and η, R_m can be calculated using Eq. (4):

$$J_{membrane} = \frac{\Delta P}{\eta R_m} \tag{4}$$

The resistance due to the deposition of foulants on the membrane surface, R_d, was calculated as follows:

$$R_d = R_t - R_m. \tag{5}$$

Schippers and Verdouw [38] developed an equation to interpret the fouling behaviour of cross-flow filtration by taking into account two fouling phenomena: pore blocking and cake formation. The proposed equation was expressed as follows:

$$\frac{t}{V} = \frac{\eta I}{2\Delta P A^2} V + \frac{\eta R_m}{\Delta P A}, \quad (6)$$

Where t is the filtration time, V is the cumulative permeate volume, η is the dynamic viscosity, I is the fouling index, ΔP is the TMP, A is the membrane area, and R_m is the membrane hydraulic resistance. The fouling index was obtained from the gradient of t/V versus V while specific cake resistance, α, is calculated as:

$$\alpha = I/C_b. \quad (7)$$

where C_b is the bulk concentration of foulant and I is the fouling index.

2.6. Analytical methods

HA absorptivity was measured using UV/Vis spectrophotometer (Lambda 35, PerkinElmer, USA) at the wavelength of 254 nm. Turbidity was measured using Turbidimeter (2100N, HACH, USA). The colloidal stability of the supernatant water after the pre-treatment coagulation process was evaluated based on the zeta potential value using Zeta-Sizer (Malvern, UK) on the basis of DLS theory and cumulant method, whereas Master-Sizer (Malvern, UK) was used to determine the particle size in the supernatant.

3. Results and Discussion

3.1. Coagulation process performance and mechanism study

Theoretically, HA molecules alone in synthetically prepared water could not be effectively deposited at the bottom of the jar if the settling process is merely relying on gravity. The

presence of electrostatic repulsion among HA molecules corresponded to the negative charges of carboxyl functional groups tends to stabilise the HA molecules in suspension. Thus, there will be less or no tendency for HA molecules to approach and agglomerate. In general, a suspension is considered stable when the zeta potential is less than -30 mV or greater than + 30 mV and particles in dispersions tend to repel each other; therefore, no agglomeration occurs [39]. In order to remove the HA molecules, coagulant is required.

In order to verify the effect of coagulant dosage on coagulation process performance and to obtain the optimum coagulant dosage for a favourable outcome, the turbidity removal and HA concentration reduction were measured. In addition, zeta potential of the supernatant water from two different coagulants; $FeCl_3$ and chitosan at different dosage were measured to predict the coagulation mechanisms involved in the removal of turbidity and HA. After a series of runs with different dosages, the range of chitosan and $FeCl_3$ dosage were narrowed down. For the sake of simplicity and clarity, only the dosages around the optimal are shown in Fig. 2. The chitosan was varied within the range of 3.5-7 mg/L, whereas the $FeCl_3$ dosage was adjusted within the range of 6-15 mg/L.

Once the coagulants had been injected into the test water, small and fluffy flocs started to form in the solution. During the slow stirring process, those flocs collided with each other and entangled into larger flocs, as shown in Fig. 3. Therefore, by referring to Fig. 2, it could be observed that the trends of turbidity and HA removal percentage versus coagulant dosage varies for both coagulants. With relatively high turbidity and HA removal, chitosan demonstrates its optimum dosage at 5.5 mg/L, which could remove 98% and 93% of turbidity and HA, respectively. On the contrary, 8 mg/L of $FeCl_3$ is required in the coagulation process to achieve 94% removal of turbidity and HA. Results from this study discovered that chitosan is as competitive as $FeCl_3$, with both coagulants successfully reducing the turbidity of the synthetic water down to less than 1 NTU, which was within the recommended working conditions for a membrane filtration unit. However, when the coagulant was added beyond this optimum dosage, the turbidity and HA removal efficiency of both coagulants started to reduce.

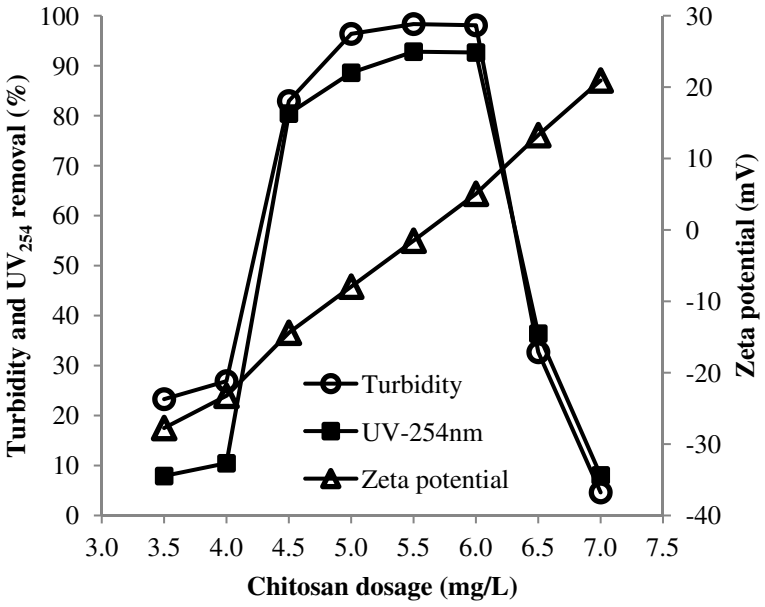

(a)

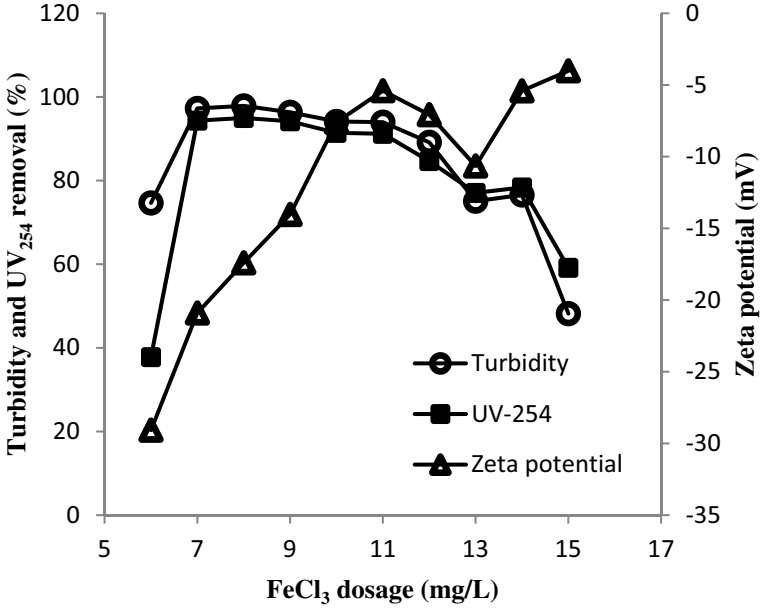

(b)

Fig. 2. Turbidity removal, HA concentration reduction, and zeta potential in (a) chitosan coagulation process, and (b) $FeCl_3$ coagulation process.

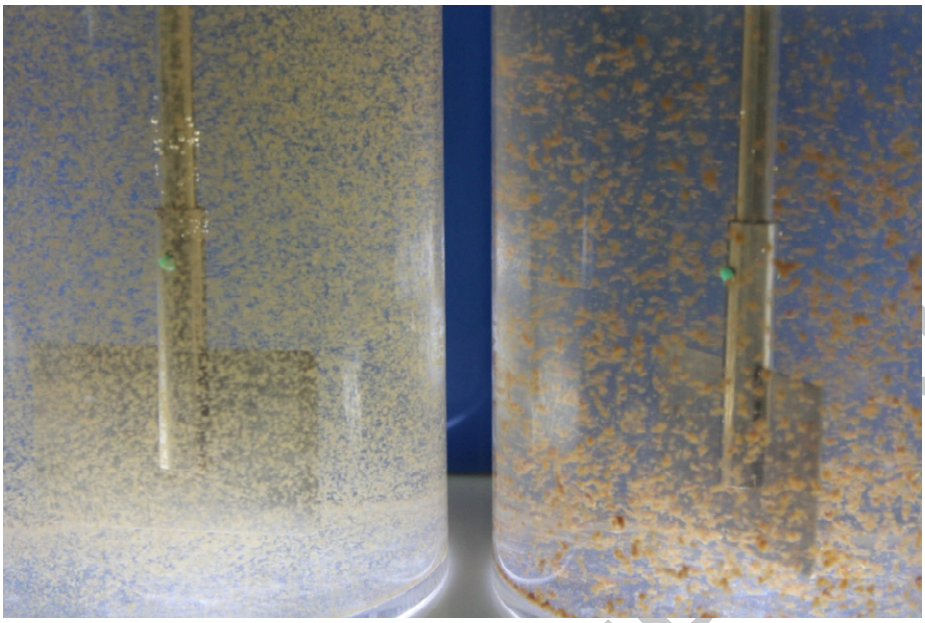

Fig. 3. Flocs formation in the chitosan coagulation process (left) and $FeCl_3$ coagulation process (right) during the slow stirring coagulation period.

Due to the variation in zeta potential values in the solution produced by each coagulant, it was postulated that different mechanisms take place in each coagulation process. Mechanisms involved in the coagulation process can be divided into two major categories: charge neutralisation/electrostatic interaction and sweep coagulation/co-precipitation [12]. The chitosan coagulation process could be explained by a charge neutralization mechanism, as shown in Fig. 4. With the addition of chitosan in the synthetic water, HA molecules started to lose stability in water suspension, as the repulsion forces between the HA molecules were reduced. This effect was due to the electrostatic shielding among the negative charges of HA molecules provided by cationic chitosan which act similarly to a binding agent of two carboxyl groups and consequently result in coagulation and particle precipitation [40,41]. This postulation was supported by the zeta potential results, as depicted in Fig. 2. At low chitosan dosage, the amount of chitosan was too little to completely neutralise all of the HA molecules in solution. The HA molecules still possess high negative charges and the resultant electrostatic repulsion between the HA molecules will prevent the formation of larger flocs, which are represented by a slight reduction in the negative zeta potential value.

In general, the increase in $FeCl_3$ dosage also leads to the reduction of negative zeta potential value. However, in contrast to chitosan, the zeta potential value of the HA-kaolin solution following the $FeCl_3$ coagulation process never reached IEP, yet still remained negative, even at the optimum dosage. The zeta potential at optimal $FeCl_3$ dosage was -17.4 mV. Since the zeta potential at the optimal $FeCl_3$ dosage was not near to zero, it can be indicated that charge neutralization was not the predominant mechanism involved in the $FeCl_3$ coagulation process. A similar conclusion was drawn by Ng et al. and Zhong et al. [12,42], where the charge neutralisation mechanism was excluded due to the negative zeta potential obtained. Instead, sweep coagulation, which involves the adsorption and entrapment of HA onto the ferric precipitates, might be the major mechanism for flocs formation in this coagulation process [17,42].

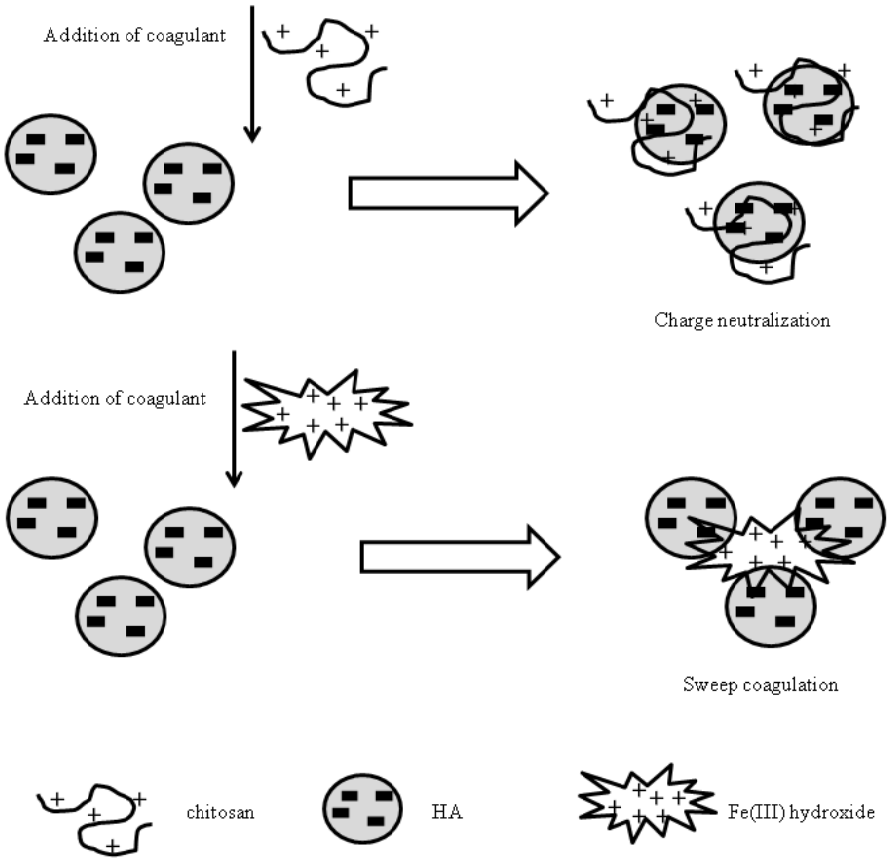

Fig. 4. Schematic diagram of coagulation mechanisms.

In the sweep coagulation mechanism, the $FeCl_3$ coagulant will undergo a hydrolysis reaction when it is dosed in synthetic water. The $FeCl_3$ coagulant hydrolysis products will eventually form precipitates when HA molecules in the synthetic water are incorporated in the hydroxide matrix, as shown in Fig. 4. At $FeCl_3$ dosages lower than 7 mg/L, an insufficient amount of $FeCl_3$ coagulant in synthetic water failed to enmesh the HA molecules in the suspension and thus resulted in extremely low turbidity and HA removal rate [43]. In contrast, for the overdose state, excessive repulsion between the ferric hydroxide in the solution might hinder it from sweeping the HA in the solution to form precipitates.

According to Jarvis et al. and Kim et al. [44,45], the flocs formed by charge neutralisation are smaller compared to sweep coagulation flocs. Our results presented in Fig. 3 agree well with these findings. It was observed that the flocs formed by sweep coagulation mechanism in $FeCl_3$ coagulation process were larger compared to the flocs formed by charge neutralisation mechanism in the chitosan coagulation process. Particle size distribution in supernatant water presented in Fig. 5 was further confirmed this claim. Fig. 5 shows that different coagulants played an important role in changing the particle size distribution of supernatant water after the coagulation process. Particle size in raw synthetic water was distributed to a broader range with a mean particle size of 5.2 µm. Although the supernatant water after the chitosan coagulation process and $FeCl_3$ coagulation process has a similar particle size distribution pattern, particle size distribution narrowing was noticed for supernatant water in both coagulation processes. It can be observed that the mean particle size of chitosan and $FeCl_3$supernatant water were shifted to 4.6 µm and 9.0 µm, respectively. The residual particles after the $FeCl_3$ coagulation process were twice the size of those from chitosan coagulation, which concur with the aforementioned claim. By referring to Fig. 5, it could be seen that the particle size of raw solution is broadly distributed while the distributions of supernatant solutions are more narrow and concentrated. It can be observed that the particle size of raw solution is skewed to the right (larger particle size), which might explain why its mean particle size is slightly larger than the particle size after chitosan coagulation process. Hence, given by the small discrepancy between the particle sizes, it can be concluded that the particle size after chitosan coagulation remained roughly the same as the raw water.

Additionally, sludge sedimentation after the coagulation processes shown in Fig. 6also further support the postulation of different mechanisms involved in each coagulation process. For sweep coagulation, Fe(III) formed precipitates thus added to the total amount of sludge produced (as observed in Fig. 6 (right)) in the $FeCl_3$ coagulation process. However, chitosan did not form hydroxide precipitates in water, thus resulting in less sludge produced in the chitosan coagulation process compared to the $FeCl_3$ coagulation process. This finding was in line with the work of Hu et al., who reported that the amount of sludge produced by aluminium coagulation was much higher than chitosan coagulation due to the formation of aluminium hydroxide flocs [11].

In a nutshell, particle size distribution in the supernatant water after the coagulation pre-treatment process is governed by the type of coagulant used and the mechanism involved in the coagulation process. The various supernatant water properties produced by different coagulation processes are expected to contribute to different membrane fouling phenomena.

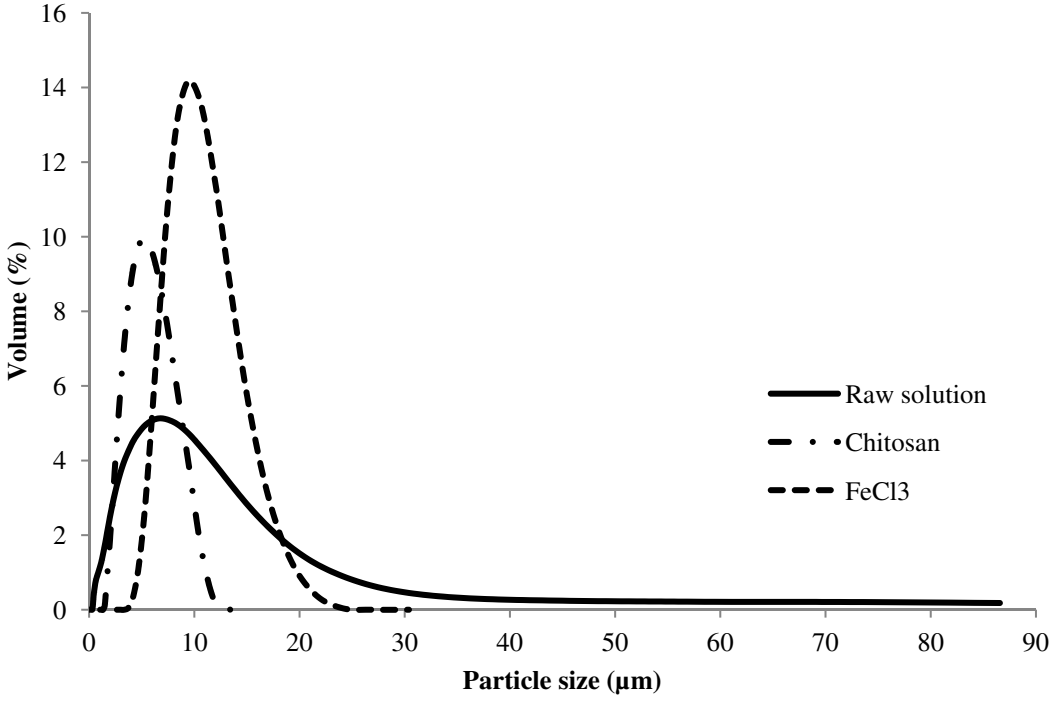

Fig. 5. Particle size distribution of synthetically prepared feed water and supernatant water from $FeCl_3$ and chitosan coagulation processes; mean particle size: 5.2 µm, 9.0 µm, and 4.6 µm, respectively.

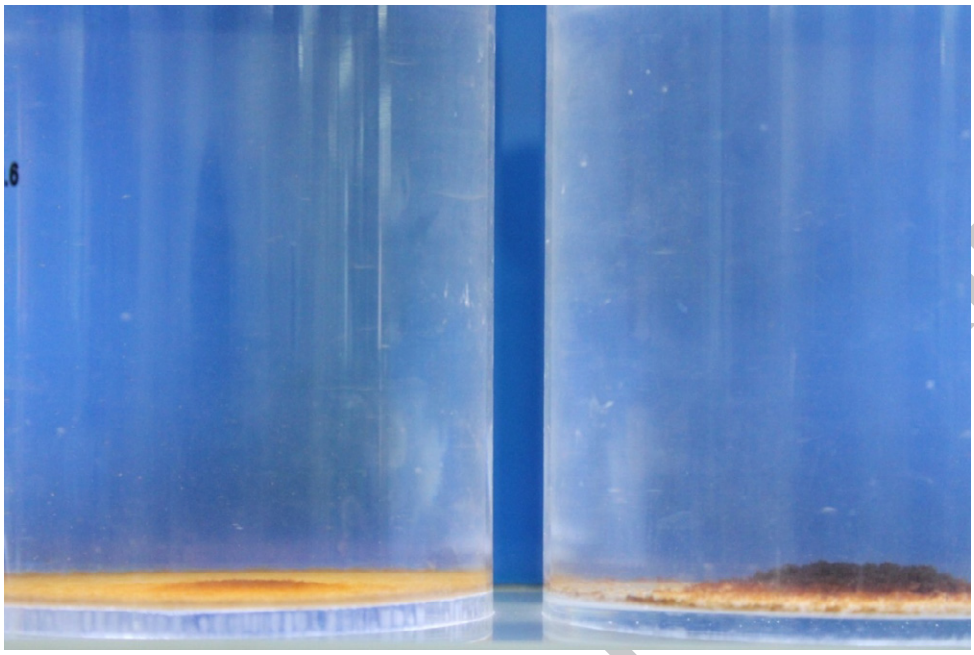

Fig. 6. Sludge sedimentation from the chitosan coagulation process (left) and $FeCl_3$ coagulation process (right).

3.2. Membrane performance and fouling

The supernatant water produced with the use of optimum dosage from both coagulation pre-treatments was followed by the membrane filtration process. The turbidity and HA concentration of the permeates produced by hybrid coagulation-membrane processes were measured; the experimental results showed that all hybrid processes in this study managed to remove nearly all of the turbidity and HA in the synthetic water to an undetectable level. In general, this study indicates that the hybrid coagulation-NF/RO processes had successfully managed to remove the HA in water.

Fig. 7 illustrates the permeate flux profiles ofNF270 and XLE membranes in treating the supernatant water from different coagulation processes. By referring to Fig. 7(a), it is clearly seen that the supernatant water pre-treated by the $FeCl_3$ coagulation process causes a very drastic initial flux decline compared to the supernatant water pre-treated by the chitosan coagulation process. After around half an hour of filtration, the flux decline in the hybrid $FeCl_3$-NF 270 process became lesser and remained almost constant for the subsequent filtration period, whereas,

for the hybrid chitosan-NF 270 process, the flux declined progressively along the filtration. Eventually, after two and a half hours of the filtration process, the flux of hybrid chitosan-NF 270 process was lower than that of the hybrid $FeCl_3$-NF 270 process. On the contrary, the flux profiles of the XLE membrane using the supernatant water from both coagulation pre-treatment processes as the feed water for the membrane process did not show any significant difference. Both membrane filtration processes depicted a sudden flux drop for the initial process, but the fluxes started to decrease gradually after a short period.

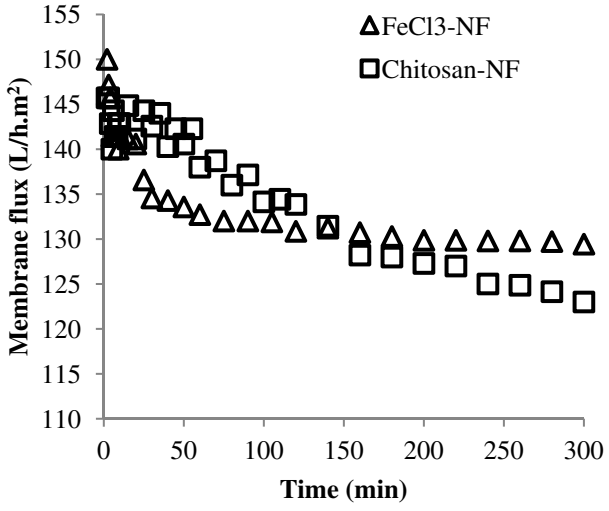

(a)

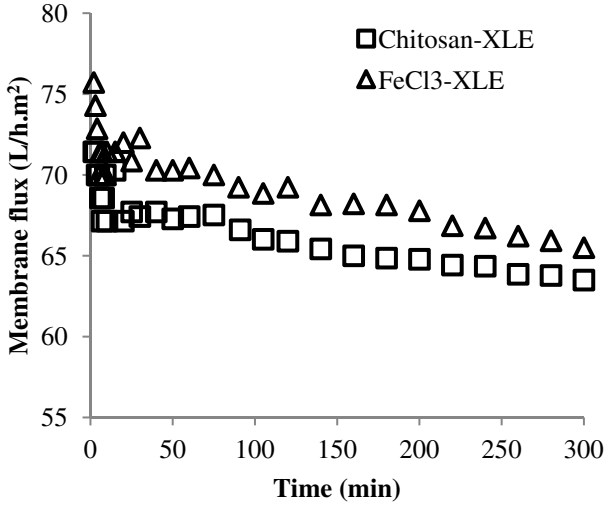

(b)

Fig. 7. Membrane permeate flux of (a) NF 270 membrane and (b) XLE membrane.

The type of coagulant used and the coagulation mechanism involved in the coagulation process will produce supernatant water with different particle sizes, structures, and zeta potential values. This will further affect the performance and fouling of the following membrane process [2,20,31,46–49]. The NF 270 membrane has high negative surface charge (-32.6 mV) at pH 7 [20]. However, the surface charge of the NF 270 membrane decreased to around -8.6 mV when it came into contact with the supernatant water from the coagulation pre-treatment process at pH 4.2±0.1 [20]. With a lower surface charge value, the charge repulsive strength of NF 270 was weakened in which the foulant had a greater chance of attaching to the membrane surface. This phenomenon was obviously seen in the hybrid chitosan-NF 270 process, where the small flocs with nearly zero charge continuously accumulated at the membrane surface and hence contributed to the gradual flux decline as shown in Fig. 7(a). A similar phenomenon was observed in the study carried out by Yu et al. [50]. The accumulation of foulant was continued for the whole filtration period due to the neutral (near zero charge) foulant layer formed which could not act as an additional barrier to the membrane. In contrast, the larger particle size of supernatant water produced from the $FeCl_3$ coagulation process will impose another additional effect at the initial stage of membrane filtration process for hybrid $FeCl_3$-NF 270 process. During the initial stage of filtration, large particles in the supernatant water rapidly deposited on the membrane surface and subsequently blocked the pores [51]. The flux was greatly shut off by the particles deposited on the membrane surface, causing an initial sharp decline in permeate flux whereby filtrate can only pass through the unblocked pore area. After some time, a bed of uniform foulant formed over the entire membrane upper surface. This fouling layer, which possessed a negative charge, will likely repel the foulant from further adsorption on the membrane surface [52]. Hence, the flux decline in hybrid $FeCl_3$-NF 270 process became lesser and remained almost constant for the subsequent filtration period.

For XLE membranes, a rapid permeate flux decline was observed at the initial filtration stage, although it only took place for a very short period. This may be attributed to the rougher surface of the XLE membrane, which plays a determinant role in membrane fouling. A coarser XLE membrane can much more easily adsorb foulants from water into the membrane valleys

compared to smoother NF270 membrane with lower surface roughness [53]. Consequently, relatively high amounts of foulant were easily adsorbed on the membrane surface, which then greatly impaired the membrane permeate flux [36,54–58]. However, the impact of supernatant water particle size on XLE membrane fouling was minimal, in which both the hybrid $FeCl_3$-XLE process and chitosan-XLE process depicted a similar fouling trend. In this practice, as the membranes were tested under same hydrodynamic conditions and the effect of foulant is minimum, the different fouling behaviour between NF270 and XLE membrane could thus be attributed to the different membrane properties.

3.3. Modified Fouling Index (MFI)

Plots of filtration time to filtration volume (t/V) ratio versus cumulative permeate volume (V) were constructed and shown in Fig. 8 to interpret the fouling behaviour of cross-flow filtration by taking into account two simultaneous fouling phenomena: pore blocking and cake formation. This model equation was successfully applied in this HA fouling study for both NF 270 and XLE membranes for the description of membrane fouling phenomena. According to Schippers and Verdouw [38], region I in the plots, which accounted for rapid t/V increment, denotes the pore blocking, while region II described the slower t/V increment as being due to the cake formation. However, the pore blocking mechanism in this context might be different from the pore blocking fouling in UF/MF membranes. Since NF/RO membranes do not have discrete pores as UF/MF membranes, the pore blocking in this study was interpreted as the flux shut off by foulant on the membrane surface, whereby filtrate can only pass through the unblocked area. It could also be attributed to the concentration polarization effect where the HA being brought to membrane surface and accumulated on it [59]. Concentration polarization played a key role in the formation of a foulant layer on the membrane surface which reduced the membrane flux.

Fig. 8(a) shows that the initial t/V value for hybrid $FeCl_3$-NF 270 process was increasing dramatically compared to the hybrid system using chitosan in the coagulation pre-treatment process. The t/V value for the hybrid chitosan-NF 270 process was gradually increasing all the way through the membrane filtration. The difference between these two hybrid systems may be attributed to the different fouling mechanism influenced by the supernatant water properties

feeding the membrane unit. The particle size in the supernatant water produced by $FeCl_3$ coagulation pre-treatment was nearly twice that of the particles from chitosan coagulation pre-treatment, as shown in Fig. 5. Hence, fast fouling occurred in hybrid $FeCl_3$-NF 270 process during the initial filtration period where large aggregates in supernatant water pre-treated by the $FeCl_3$ coagulation process were easily attached to the membrane surface, resulting in the quick build-up of foulant layer on the membrane surface [60]. However, the chitosan coagulation pre-treatment process produced supernatant water with smaller particles which will not cover up the membrane surface as fast as the large particles in supernatant water pre-treated with the $FeCl_3$ coagulation process. Since the particles in the supernatant water pre-treated by the chitosan coagulation process were neutral in charge (as reported in Fig. 2), the deposition of foulant on the membrane surface was continuing. A similar observation was reported by Bergamasco et al. [31] when investigating the fouling behaviour of the UF membrane by chitosan and aluminium sulphate coagulants.

Besides, it was observed that the hybrid coagulation-XLE processes depicted a similar trend in region I as the hybrid $FeCl_3$-NF 270 process, but with a higher t/V value. The t/V value of a membrane filtration process is dominated by the function of R_m, which depended on the membrane property. As XLE is an RO membrane, a tighter XLE membrane structure will likely induce a higher R_m value, thereby contributing to a higher t/V value. However, a contradictory trend was observed in the hybrid coagulation-XLE process, in which the hybrid chitosan-XLE process had a higher t/V value compared to the hybrid $FeCl_3$–XLE process. It is believed that a coarser XLE membrane with ridge-and-valley created across the membrane area much more easily entrapped smaller particles in supernatant water produced by chitosan coagulation pre-treatment process in the membrane valleys. Consequently, relatively large amounts of particles have been adsorbed, provided with extra hydraulic resistance. This eventually led to poorer fouling possessions and thus coherence to a higher t/V value in the hybrid chitosan-XLE process. This finding showed that the physical properties of the membrane are pronounced in terms of membrane fouling.

For all hybrid coagulation-membrane processes, foulant was progressively deposited on the membrane surface and after a period, a bed of uniform solute was formed over the entire

membrane upper surface. This cake layer on the membrane surface can act as an additional barrier to the membrane process which prevented the further deposition of foulant and therefore contributes to a higher and more stable t/V value (as depicted by region II).

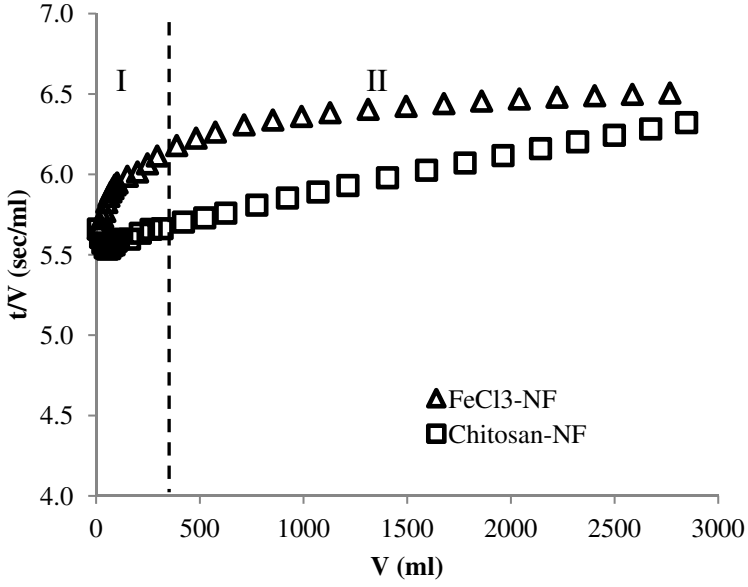

(a)

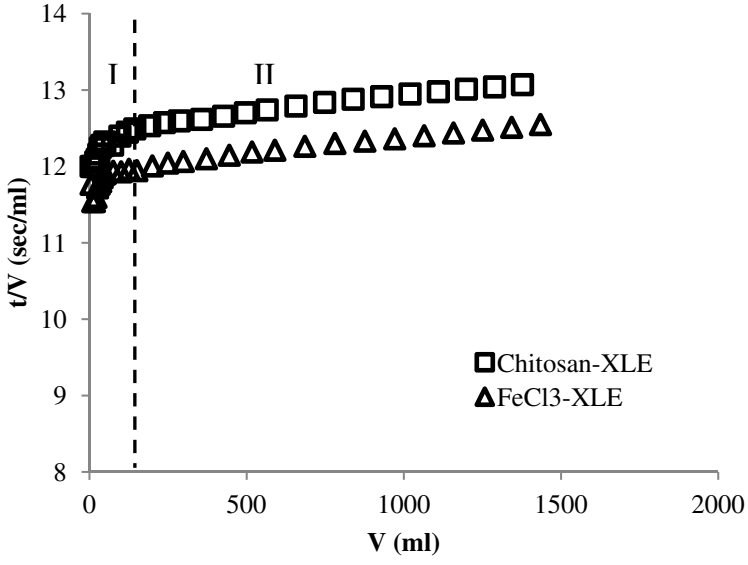

(b)

Fig. 8. Filtration time to filtration volume ratio versus cumulative permeate volume for (a) NF 270 membrane system and (b) XLE membrane system.

3.4. Extraction of foulant adsorbed on the membranes

In this study, membrane cleaning was studied by chemical cleaning, which involved soaking the membranes in 0.1 M NaOH solution to extract the foulant that was deposited on the membrane surface during the membrane filtration process. The amount of foulant extracted from the membrane surfaces was measured in terms of UV_{254} absorbance and compared. The UV_{254} absorbance of the extractions from each hybrid coagulation-membrane process reported in Table 3 was divided by the membrane surface area to signify the amount of foulant deposited per unit membrane surface area.

Overall, the UV_{254} absorbance/membrane surface area value for the compounds extracted from the membranes using chitosan coagulation as a pre-treatment process was found to be relatively higher than the $FeCl_3$ coagulation process. The higher amount of foulant deposited on the membrane surface using chitosan coagulation in the pre-treatment process might be attributed to the smaller particle size in chitosan pre-treated supernatant water that can completely cover the membrane surface. Besides, the particles in the chitosan pre-treated supernatant solution were neutral in charge. Hence, the foulant were more readily to adsorb onto the membrane surface since electrostatic repulsion acting on them was minimal, compared to the negatively charged particles from $FeCl_3$ coagulation process.

Furthermore, it was observed that the foulant deposited on the membrane surface of chitosan hybrid processes was not completely dissolved by NaOH. This observation indicates that the foulant from the chitosan coagulation pre-treatment process formed a more compact (lower porosity) foulant layer on the membrane surface, which is most likely due to smaller particles in pre-treated supernatant water that were strongly bound to the membrane surface with van der Waals forces [61].

Direct evidence of specific cake resistance analysis in Table 4, which was calculated using Eq. (4), has further supported the compactness of the foulant layer on the membrane surface

from the chitosan coagulation pre-treatment process. In general, hybrid chitosan-membrane processes have higher specific cake resistance compared to hybrid $FeCl_3$-membrane processes. Previous studies performed by many researchers have reported that higher specific cake resistance resulted from the more compact foulant layer on the membrane surface [49,62].

On the contrary, the $FeCl_3$ coagulation pre-treatment process which produced larger particles compared to the chitosan coagulation pre-treatment process resulted in the formation of a higher porosity foulant layer on the membrane surface. Foulant layer with higher porosity was loosely bound to the membrane and thus easier to be removed by NaOH. The experimental results published by Yu et al. [50] agree with our findings. They discovered that larger particles formed by *in situ* Fe(III) coagulant resulted in a more porous cake layer on the membrane surface and was beneficial in reducing membrane fouling.

In a nutshell, chitosan and $FeCl_3$ coagulants produced different particle sizes in the supernatant water which eventually resulted in the variation of membrane fouling propensity. Particles in supernatant water using $FeCl_3$ coagulant were larger in size and caused a lower membrane fouling tendency compared to coagulation processes using a chitosan coagulant.

Table 3
UV_{254} absorbance of the extractions from each hybrid coagulation-membrane process

Hybrid process	UV_{254} absorbance (cm^{-1})	UV_{254} absorbance/Membrane surface area	Observation
Chitosan-NF 270	0.0763	0.1908	Not all removed
$FeCl_3$-NF 270	0.0890	0.1854	Easily removed
Chitosan-XLE	0.1006	0.1829	Not all removed
$FeCl_3$-XLE	0.0788	0.1251	Easily removed

Table 4
Specific cake resistance values of the hybrid processes

Hybrid process	Specific cake resistance, $\times 10^{-5}$ (m^3/kg)
$FeCl_3$-NF 270	2.4624
Chitosan-NF 270	8.0495
$FeCl_3$-XLE	14.0609
Chitosan-XLE	14.3625

4. Conclusions

In conclusion, the results obtained in this study indicated that the hybrid coagulation-membrane processes were capable of removing nearly all turbidity and HA concentrations in the water. Chitosan and $FeCl_3$ coagulants were efficient at reducing the foulant in synthetic solution and producing supernatant water with a quality that was acceptable for membrane operation. However, the coagulation mechanisms attributed by each coagulant were different and this affected the membrane performance in the hybrid system. Although chitosan was as competent as $FeCl_3$, hybrid chitosan-NF 270 membrane process did not perform as well as $FeCl_3$-NF 270 membrane processes, in which hybrid chitosan-NF 270 membrane process showed more severe membrane fouling propensity due to the smaller particle sizes of the supernatant water produced by the chitosan coagulation pre-treatment process. Whereas, the impact of supernatant water particle size after chitosan and $FeCl_3$ coagulation pre-treatment processes on XLE membrane fouling was minimal as for XLE membrane, rougher surface structure plays a dominant role in attributing to the membrane fouling. Based on the findings in this study, it is strongly recommended that the selection of a coagulant is crucial in hybrid coagulation-membrane treatment processes to attain high removal efficiency and high fouling mitigation. Further studies are suggested to gain more insightful details about the fouling problem and hybrid coagulation-membrane process.

Acknowledgments

This paper was made possible by NPRP grant #[5-1425-2-607] from the Qatar National Research Fund (a member of Qatar Foundation). The statements made herein are solely the responsibility of the author[s]. The authors also wish to acknowledge the Ministry of Education Malaysia for sponsoring W.L. Ang's postgraduate study via MyBrain.

References

[1] V. Kazpard, B.S. Lartiges, C. Frochot, J.B. d'Espinose de la Caillerie, M.L. Viriot, J.M. Portal, et al., Fate of coagulant species and conformational effects during the aggregation

of a model of a humic substance with Al13 polycations, Water Res. 40 (2006) 1965–74. doi:10.1016/j.watres.2006.03.014.

[2] L. Rizzo, A. Di Gennaro, M. Gallo, V. Belgiorno, Coagulation/chlorination of surface water: A comparison between chitosan and metal salts, Sep. Purif. Technol. 62 (2008) 79–85. doi:10.1016/j.seppur.2007.12.020.

[3] EPA, Disinfection Byproduct Health Effects, (2011). http://www.epa.gov/envirofw/html/icr/dbp_health.html.

[4] P. Jarvis, B. Jefferson, S. Parsons, Breakage, regrowth, and fractal nature of natural organic matter flocs, Environ. Sci. Technol. 39 (2005) 2307–2314.

[5] F. Renault, B. Sancey, P.-M. Badot, G. Crini, Chitosan for coagulation/flocculation processes – An eco-friendly approach, Eur. Polym. J. 45 (2009) 1337–1348. doi:10.1016/j.eurpolymj.2008.12.027.

[6] J. Wei, B. Gao, Q. Yue, Y. Wang, W. Li, X. Zhu, Comparison of coagulation behavior and floc structure characteristic of different polyferric-cationic polymer dual-coagulants in humic acid solution., Water Res. 43 (2009) 724–32. doi:10.1016/j.watres.2008.11.004.

[7] Z.L. Yang, B.Y. Gao, Q.Y. Yue, Y. Wang, Effect of pH on the coagulation performance of Al-based coagulants and residual aluminum speciation during the treatment of humic acid-kaolin synthetic water., J. Hazard. Mater. 178 (2010) 596–603. doi:10.1016/j.jhazmat.2010.01.127.

[8] Y. Wang, B.-Y. Gao, X.-M. Xu, W.-Y. Xu, The effect of total hardness and ionic strength on the coagulation performance and kinetics of aluminum salts to remove humic acid, Chem. Eng. J. 160 (2010) 150–156. doi:10.1016/j.cej.2010.03.028.

[9] S. Zhao, B. Gao, Y. Wang, Z. Yang, Influence of a new coagulant aid-Enteromorpha extract on coagulation performance and floc characteristics of aluminum sulfate coagulant in kaolin–humic acid solution treatment, Colloids Surfaces A Physicochem. Eng. Asp. 417 (2013) 161–169. doi:10.1016/j.colsurfa.2012.10.062.

[10] G. Crini, P.-M. Badot, Application of chitosan, a natural aminopolysaccharide, for dye removal from aqueous solutions by adsorption processes using batch studies: A review of recent literature, Prog. Polym. Sci. 33 (2008) 399–447. doi:10.1016/j.progpolymsci.2007.11.001.

[11] C.-Y. Hu, S.-L. Lo, C.-L. Chang, F.-L. Chen, Y.-D. Wu, J. Ma, Treatment of highly turbid water using chitosan and aluminum salts, Sep. Purif. Technol. 104 (2013) 322–326. doi:10.1016/j.seppur.2012.11.016.

[12] M. Ng, S. Liu, C.W.K. Chow, M. Drikas, R. Amal, M. Lim, Understanding effects of water characteristics on natural organic matter treatability by PACl and a novel PACl-

chitosan coagulants., J. Hazard. Mater. 263 (2013) 718–25. doi:10.1016/j.jhazmat.2013.10.036.

[13] M.B. Zakaria, W.M.W. Muda, M.P. Abdullah, Chitin and Chitosan The Versatile Environmentally Friendly Modern Materials, 1st ed., Penerbit UKM, Malaysia, 1995.

[14] R. Divakaran, V.. Sivasankara Pillai, Flocculation of kaolinite suspensions in water by chitosan, Water Res. 35 (2001) 3904–3908. doi:10.1016/S0043-1354(01)00131-2.

[15] L. Rizzo, G. Lofrano, M. Grassi, V. Belgiorno, Pre-treatment of olive mill wastewater by chitosan coagulation and advanced oxidation processes, Sep. Purif. Technol. 63 (2008) 648–653. doi:10.1016/j.seppur.2008.07.003.

[16] J. Ruhsing Pan, C. Huang, S. Chen, Y.-C. Chung, Evaluation of a modified chitosan biopolymer for coagulation of colloidal particles, Colloids Surfaces A Physicochem. Eng. Asp. 147 (1999) 359–364. doi:10.1016/S0927-7757(98)00588-3.

[17] S. Bratskaya, S. Schwarz, D. Chervonetsky, Comparative study of humic acids flocculation with chitosan hydrochloride and chitosan glutamate., Water Res. 38 (2004) 2955–61. doi:10.1016/j.watres.2004.03.033.

[18] W.L. Ang, A.W. Mohammad, N. Hilal, C.P. Leo, A review on the applicability of integrated/hybrid membrane processes in water treatment and desalination plants, Desalination. (2014). http://dx.doi.org/10.1016/j.desal.2014.03.008.

[19] K.-V. Peinemann, S.P. Nunes, Membranes for Water Treatment, Wiley-VCH Verlag GmbH & Co. KGaA, 2010.

[20] K. Listiarini, J.T. Tor, D.D. Sun, J.O. Leckie, Hybrid coagulation–nanofiltration membrane for removal of bromate and humic acid in water, J. Memb. Sci. 365 (2010) 154–159. doi:10.1016/j.memsci.2010.08.048.

[21] A. Gorenflo, F.H. Frimmel, D. Velazquez-Padron, Nanofiltration of a German groundwater of high hardness and NOM content : performance and costs, Desalination. 1 (2002) 253–265.

[22] J.E. Kilduff, S. Mattaraj, A. Wigton, M. Kitis, T. Karanfil, Effects of reverse osmosis isolation on reactivity of naturally occurring dissolved organic matter in physicochemical processes., Water Res. 38 (2004) 1026–36. doi:10.1016/j.watres.2003.10.049.

[23] F.H. Butt, F. Rahman, U. Baduruthamal, Characterization of foulants by autopsy of RO desalination membranes, Desalination. 114 (1997) 51–64. doi:10.1016/S0011-9164(97)00154-9.

[24] S. Xia, X. Li, Q. Zhang, B. Xu, G. Li, Ultrafiltration of surface water with coagulation pretreatment by streaming current control, Desalination. 204 (2007) 351–358. doi:10.1016/j.desal.2006.03.544.

[25] C.-W. Jung, H.-J. Son, L.-S. Kang, Effects of membrane material and pretreatment coagulation on membrane fouling: fouling mechanism and NOM removal, Desalination. 197 (2006) 154–164. doi:10.1016/j.desal.2005.12.022.

[26] Q. Xiangli, Z. Zhenjia, W. Nongcun, V. Wee, M. Low, C.S. Loh, et al., Coagulation pretreatment for a large-scale ultrafiltration process treating water from the Taihu River, Desalination. 230 (2008) 305–313. doi:10.1016/j.desal.2007.11.032.

[27] P.C. Kampa, J.C. Kruithofb, H.C. Folmer, UF / RO treatment plant Heemskerk : from challenge to full scale application, Desalination. 1 (2000) 27–35.

[28] J.H. Kweon, H.-W. Hur, G.-T. Seo, T.-R. Jang, J.-H. Park, K.Y. Choi, et al., Evaluation of coagulation and PAC adsorption pretreatments on membrane filtration for a surface water in Korea: A pilot study, Desalination. 249 (2009) 212–216. doi:10.1016/j.desal.2008.08.014.

[29] K. Konieczny, D. Sąkol, J. Płonka, M. Rajca, M. Bodzek, Coagulation—ultrafiltration system for river water treatment, Desalination. 240 (2009) 151–159. doi:10.1016/j.desal.2007.11.072.

[30] Y. Chen, B.Z. Dong, N.Y. Gao, J.C. Fan, Effect of coagulation pretreatment on fouling of an ultrafiltration membrane, Desalination. 204 (2007) 181–188. doi:10.1016/j.desal.2006.04.029.

[31] R. Bergamasco, L.C. Konradt-Moraes, M.F. Vieira, M.R. Fagundes-Klen, A.M.S. Vieira, Performance of a coagulation–ultrafiltration hybrid process for water supply treatment, Chem. Eng. J. 166 (2011) 483–489. doi:10.1016/j.cej.2010.10.076.

[32] J. Moon, M.-S. Kang, J.-L. Lim, C.-H. Kim, H.-D. Park, Evaluation of a low-pressure membrane filtration for drinking water treatment: pretreatment by coagulation/sedimentation for the MF membrane, Desalination. 247 (2009) 271–284. doi:10.1016/j.desal.2008.12.030.

[33] N. Lee, G. Amy, J.-P. Croué, Low-pressure membrane (MF/UF) fouling associated with allochthonous versus autochthonous natural organic matter., Water Res. 40 (2006) 2357–68. doi:10.1016/j.watres.2006.04.023.

[34] X. Guo, Z. Zhang, L. Fang, L. Su, Study on ultrafiltration for surface water by a polyvinylchloride hollow fiber membrane, Desalination. 238 (2009) 183–191. doi:10.1016/j.desal.2007.11.064.

[35] www.filmtec.com, (n.d.).

[36] C.Y. Tang, Y.-N. Kwon, J.O. Leckie, Effect of membrane chemistry and coating layer on physiochemical properties of thin film composite polyamide RO and NF membranes: II. Membrane physiochemical properties and their dependence on polyamide and coating layers, Desalination. 242 (2009) 168–182.

[37] A.I. Schafer, A.. Fane, T.D. Waite, Nanofiltration-Principles and Application, 1st ed., Elsevier Science, Oxford, 2005.

[38] J.C. Schippers, J. Verdouw, The modified fouling index, a method of determining the fouling characteristics of water, Desalination. 32 (1980) 137–148.

[39] Zetasizer Nano User Manual, Malvern Instruments, 2007.

[40] M. Terashima, S. Tanaka, M. Fukushima, Coagulation characteristics of humic acid modified with glucosamine or taurine., Chemosphere. 69 (2007) 240–6. doi:10.1016/j.chemosphere.2007.04.012.

[41] J.-M. Siéliéchi, B.S. Lartiges, G.J. Kayem, S. Hupont, C. Frochot, J. Thieme, et al., Changes in humic acid conformation during coagulation with ferric chloride: implications for drinking water treatment., Water Res. 42 (2008) 2111–23. doi:10.1016/j.watres.2007.11.017.

[42] R. Zhong, X. Zhang, F. Xiao, X. Li, Z. Cai, Effects of humic acid on physical and hydrodynamic properties of kaolin flocs by particle image velocimetry., Water Res. 45 (2011) 3981–90. doi:10.1016/j.watres.2011.05.006.

[43] M.& E. Inc, G. Tchobanoglous, F.L. Burton, H.D. Stensel, Wastewater Engineering Treatment and Reuse, 4th ed., McGraw-Hill, 2004.

[44] P. Jarvis, B. Jefferson, S. a Parsons, Floc structural characteristics using conventional coagulation for a high doc, low alkalinity surface water source., Water Res. 40 (2006) 2727–37. doi:10.1016/j.watres.2006.04.024.

[45] S.-H. Kim, B.-H. Moon, H.-I. Lee, Effects of pH and dosage on pollutant removal and floc structure during coagulation, Microchem. J. 68 (2001) 197–203.

[46] A.G. Fane, T.D. Waite, A.I. Scha, Cost factors and chemical pretreatment effects in the membrane filtration of waters containing natural organic matter, Water Res. 35 (2001) 1509–1517.

[47] W. Yu, N. Graham, H. Liu, J. Qu, Comparison of FeCl3 and alum pre-treatment on UF membrane fouling, Chem. Eng. J. 234 (2013) 158–165. doi:10.1016/j.cej.2013.08.105.

[48] J.-L. Lin, C. Huang, J.R. Pan, D. Wang, Effect of Al(III) speciation on coagulation of highly turbid water., Chemosphere. 72 (2008) 189–96. doi:10.1016/j.chemosphere.2008.01.062.

[49] J. Wang, J. Guan, S.R. Santiwong, T.D. Waite, Characterization of floc size and structure under different monomer and polymer coagulants on microfiltration membrane fouling, J. Memb. Sci. 321 (2008) 132–138. doi:10.1016/j.memsci.2008.04.008.

[50] W. Yu, N. Graham, H. Liu, H. Li, J. Qu, Membrane fouling by Fe-Humic cake layers in nano-scale: Effect of in-situ formed Fe(III) coagulant, J. Memb. Sci. 431 (2013) 47–54. doi:10.1016/j.memsci.2012.12.035.

[51] E.-S. Kim, Y. Liu, M. Gamal El-Din, The effects of pretreatment on nanofiltration and reverse osmosis membrane filtration for desalination of oil sands process-affected water, Sep. Purif. Technol. 81 (2011) 418–428. doi:10.1016/j.seppur.2011.08.016.

[52] M.U. Polina Dobromirova Peeva, Aisyah Endah Palupi, Ultrafiltration of humic acid solutions through unmodified and surface functionalized low-fouling polyethersulfone membranes – Effects of feed properties, molecular weight cut-off and membrane chemistry on fouling behavior and cleanability, Sep. Purif. Technol. 81 (2011) 124–133.

[53] X. Cao, J. Ma, X. Shi, Z. Ren, Effect of TiO2 nanoparticle size on the performance of PVDF membrane, Appl. Surf. Sci. 253 (2006) 2003–2010. doi:10.1016/j.apsusc.2006.03.090.

[54] C.Y. Tang, Y. Kwon, J.O. Leckie, Effect of membrane chemistry and coating layer on physiochemical properties of thin film composite polyamide RO and NF membranes I . FTIR and XPS characterization of polyamide and coating layer chemistry, Desalination. 242 (2009) 149–167. doi:10.1016/j.desal.2008.04.003.

[55] Y. Wang, C.Y. Tang, Protein fouling of nanofiltration , reverse osmosis , and ultrafiltration membranes — The role of hydrodynamic conditions , solution chemistry , and membrane properties, J. Memb. Sci. 376 (2011) 275–282. doi:10.1016/j.memsci.2011.04.036.

[56] G. Hurwitz, G.R. Guillen, E.M.V. Hoek, Probing polyamide membrane surface charge, zeta potential, wettability, and hydrophilicity with contact angle measurements, J. Memb. Sci. 349 (2010) 349–357. doi:10.1016/j.memsci.2009.11.063.

[57] E.M. Vrijenhoek, S. Hong, M. Elimelech, Influence of membrane surface properties on initial rate of colloidal fouling of reverse osmosis and nanofiltration membranes, J. Memb. Sci. 188 (2001) 115–128. doi:10.1016/S0376-7388(01)00376-3.

[58] J.S. Louie, I. Pinnau, I. Ciobanu, K.P. Ishida, A. Ng, M. Reinhard, Effects of polyether-polyamide block copolymer coating on performance and fouling of reverse osmosis membranes, J. Memb. Sci. 280 (2006) 762–770.

[59] W. Yuan, A.L. Zydney, Humic acid fouling during microfiltration, J. Memb. Sci. 157 (1999) 1–12. doi:10.1016/S0376-7388(98)00329-9.

[60] H. Kim, J. Choi, S. Takizawa, Comparison of initial filtration resistance by pretreatment processes in the nanofiltration for drinking water treatment, Sep. Purif. Technol. 56 (2007) 354–362. doi:10.1016/j.seppur.2007.02.016.

[61] W.J.C. van de Ven, K. van't Sant, I.G.M. Pünt, a. Zwijnenburg, a. J.B. Kemperman, W.G.J. van der Meer, et al., Hollow fiber dead-end ultrafiltration: Axial transport variations during humic acid filtration, J. Memb. Sci. 314 (2008) 112–122. doi:10.1016/j.memsci.2008.01.035.

[62] K. Listiarini, D.D. Sun, J.O. Leckie, Organic fouling of nanofiltration membranes: Evaluating the effects of humic acid, calcium, alum coagulant and their combinations on the specific cake resistance, J. Memb. Sci. 332 (2009) 56–62. doi:10.1016/j.memsci.2009.01.037.

Highlights

- Performance and mechanism of chitosan and $FeCl_3$ coagulation processes were studied.
- Both coagulants were competitive in removing turbidity and HA in synthetic water.
- Effect of chitosan and $FeCl_3$ coagulation on NF/RO membrane fouling was investigated.
- Chitosan resulted in more severe flux decline and membrane fouling issue.
- Membrane fouling phenomena for all the hybrid processes were discussed.